ЖЭТФ, 2004, том 125, вып. 4, стр. 938–956

DYNAMICAL TUNNELING OF BOUND SYSTEMS THROUGH A POTENTIAL BARRIER: COMPLEX WAY TO THE TOP

F. Bezrukov [a*], ***D. Levkov*** [a,b**]

[a] *Institute for Nuclear Research, Russian Academy of Sciences*
117312, Moscow, Russia

[b] *Moscow State University, Department of Physics*
119899, Moscow, Russia

Submitted 15 January, 2003

A semiclassical method of complex trajectories for the calculation of the tunneling exponent in systems with many degrees of freedom is further developed. It is supplemented with an easily implementable technique that enables one to single out the physically relevant trajectory from the whole set of complex classical trajectories. The method is applied to semiclassical transitions of a bound system through a potential barrier. We find that the properties of physically relevant complex trajectories are qualitatively different in the cases of potential tunneling at low energy and dynamical tunneling at energies exceeding the barrier height. Namely, in the case of high energies, the physically relevant complex trajectories describe tunneling via creation of a state close to the top of the barrier. The method is checked against exact solutions of the Schrödinger equation in a quantum mechanical system of two degrees of freedom.

PACS: 03.65.Sq, 03.65.-w, 03.65.Xp

1. INTRODUCTION

Semiclassical methods provide a useful tool for the study of nonperturbative processes. Tunneling phenomena represent one of the most notable cases where semiclassical techniques are used to obtain otherwise unattainable information on the dynamics of the transition. A standard example of the semiclassical technique is the WKB approximation to tunneling in quantum mechanics of one degree of freedom. In this case, solutions $S(q)$ of the Hamilton–Jacobi equation are purely imaginary in the classically forbidden region. Therefore, the function $S(q)$ can be obtained as the action functional on a real trajectory $q(\tau)$, which is a solution of the equations of motion in the Euclidean time domain,

$$t = -i\tau,$$

with the real Euclidean action

$$S_E = -iS.$$

This simple picture of tunneling is no longer valid for systems with many degrees of freedom, where solutions $S(\mathbf{q})$ of the Hamilton–Jacobi equation are known to be generically complex in the classically forbidden region (see Refs. [1, 2] for a recent discussion). This leads to the concept of «mixed» tunneling, as opposed to «pure» tunneling where $S(\mathbf{q})$ is purely imaginary. «Mixed» tunneling cannot be described by any real tunneling trajectory. However, it can be related to a complex trajectory, in which case the function $S(\mathbf{q})$ (and therefore the exponential part of the wave function) is calculated as the action functional on this complex trajectory.

A particularly difficult situation arises when one considers transitions of a nonseparable system with a strong interaction between its degrees of freedom, such that the quantum numbers of the system change considerably during the transition. Methods based on the adiabatic expansion are not applicable in this situation, while the method of complex trajectories proves to be extremely useful.

The method of complex trajectories in the form suitable for the calculation of S-matrix elements was

*E-mail: fedor@ms2.inr.ac.ru
**E-mail: levkov@ms2.inr.ac.ru

formulated and checked by direct numerical calculations in Refs. [3, 4, 5] (see Ref. [6] for a review). Further studies [7–12] showed that this method can be generalized to the calculation of the tunneling wave functions and tunneling probabilities, energy splittings in double-well potentials, and decay rates from metastable states. Similar methods were successful in the study of tunneling in high-energy collisions in field theory [13–16], where one considers systems with a definite particle number ($\mathcal{N} = 2$) in the initial state, and in the study of chemical reactions and atom ionization processes, where the initial bound systems are in definite quantum states [6, 17, 18], etc. The main advantage of the method of complex trajectories is that it can be easily generalized and numerically implemented in the cases of a large and even infinite (field theory) number of the degrees of freedom, in contrast to other methods such as the Huygens-type construction in Refs. [1, 2] and the initial value representation (IVR) in Refs. [3, 19–23].

In this paper, we develop the method of complex trajectories further. Namely, we concentrate on the following problem. It is known [3] that a physically relevant complex trajectory satisfies the classical equations of motion with certain boundary conditions. However, this boundary value problem generically has also an infinite, although discrete, set of unphysical solutions. In one-dimensional quantum mechanics, all solutions can easily be classified. In systems with many degrees of freedom, such a classification is extremely difficult, if at all possible. In the case of a small number of the degrees of freedom (realistically, $N = 2$), one can scan over all solutions and find the solution giving the largest tunneling probability [3, 9, 10], but in systems with a large or infinite number of the degrees of freedom, the problem of choosing the physically relevant solution becomes a formidable task.

The problem of choosing the appropriate solution becomes even more pronounced when the qualitative properties of the relevant complex trajectory are different in different energy regions. This may happen when the physically relevant classical solution «meets» an unphysical one at some energy value $E = E_1$, or in other words, when solutions of the boundary value problem, viewed as functions of the energy, bifurcate at $E = E_1$.

In this paper, we give an example of this type, which appears to be fairly generic (see also [11, 12, 24, 15, 16]). We then develop a method that allows choosing the phyisically relevant solution automatically, implement it numerically, and check this method against the numerical solution of the full Schrödinger equation.

We study inelastic transitions of a bound system through a potential barrier. To be specific, we consider a model with one internal degree of freedom in addition to the center-of-mass coordinate. We consider a situation where the spacing between the levels of the bound system is small compared to the height of the barrier, and assume a sufficiently strong coupling between the degrees of freedom, to make sure that the quantum numbers of the bound system change considerably during the transition process. This is precisely the situation in which the method of complex trajectories shows its full strength.

Transitions of bound systems involve a particular energy scale, the barrier height V_0. At energies below V_0, classical over-barrier transitions are forbidden energetically; the corresponding regime is called «potential tunneling». For $E > V_0$, it is energetically allowed for the system to evolve classically to the other side of the barrier. However, over-barrier transitions may be forbidden dynamically even at $E > V_0$. Indeed, inelastic interactions of a bound system with a potential barrier generally lead to the excitation of the internal degrees of freedom with the simultaneous decrease of the center-of-mass energy, which may prevent the system from the over-barrier transition. The tunneling regime at energies exceeding the barrier height is called «dynamical tunneling»[1)].

Examples of dynamical tunneling are well-known in scattering theory [4]. This type of tunneling between bound states was discovered in Ref. [25], and the generality of dynamical tunneling in large molecules was stressed in Refs. [26, 27]. Dynamical tunneling is of primary interest in our study.

We observe a novel phenomenon that dynamical tunneling at $E \gtrsim V_0$ (more precisely, at $E > E_1$, where E_1 is somewhat larger than V_0) occurs in the following way: the system jumps on top of the barrier and restarts its classical evolution from the region near the top. From the physical standpoint, this is not quite what is normally meant by «tunneling through a barrier». Yet the transitions remain exponentially suppressed, but the reason is different: to jump above the barrier, the system has to undergo considerable rearrangement, unless the incoming state is chosen in a

[1)] It is clear that the properties of transitions of a bound system at $E > V_0$ depend on the choice of the initial state. Namely, there always exists a certain class of states transitions from which are not exponentially suppressed. To construct an example, one places the bound system on top of the barrier and evolves it classically backwards in time to the region where the interaction with the barrier is negligibly small. On the other hand, even at $E > V_0$, there are states transitions from which are exponentially suppressed (dynamical tunneling).

special way (see footnote 1). This rearrangement costs an exponentially small probability factor. We note that a similar exponential factor was argued to appear in various field theory processes with multi-particle final states [28–31].

We find that the new physical behavior of the system is related to a bifurcation of the family of complex-time classical solutions, viewed as functions of energy. This is precisely the bifurcation mentioned above. Our method of dealing with this bifurcation is to regularize the boundary value problem such that the bifurcations disappear altogether (at real energies), and the only solutions recovered after removing the regularization are physical ones.

This paper is organized as follows. The system to be discussed in what follows is introduced in Sec. 2.1. In Sec. 2.2, we formulate the boundary value problem for the calculation of the tunneling exponent. In Sec. 2.3, we then examine the classical over-barrier solutions and find all initial states that lead to classically allowed transitions. In Sec. 2.4, we present a straightforward application of the semiclassical technique outlined in Sec. 2.2 and find that it ceases to produce relevant complex trajectories in a certain region of initial data, namely, at $E > E_1$. In Sec. 3, we introduce our regularization technique and show that it indeed enables us to find all the relevant complex trajectories, including those with $E > E_1$ (Sec. 3.1). We check our method against the numerical solution of the full Schrödinger equation in Sec. 3.2. In Sec. 3.3 and Appendix C, we show how our regularization technique is used to smoothly join the «classically allowed» and «classically forbidden» families of solutions in the respective cases of two- and one-dimensional quantum mechanics.

2. SEMICLASSICAL TRANSITIONS THROUGH A POTENTIAL BARRIER

2.1. The model

The situation discussed in this paper is a transition through a potential barrier of the bound system considered in Refs. [11, 12], namely the system made of two particles of identical masses m, moving in one dimension and bound by a harmonic oscillator potential of frequency ω (Fig. 1). One of the particles interacts with a repulsive potential barrier. The potential barrier is assumed to be high and wide, while the spacing

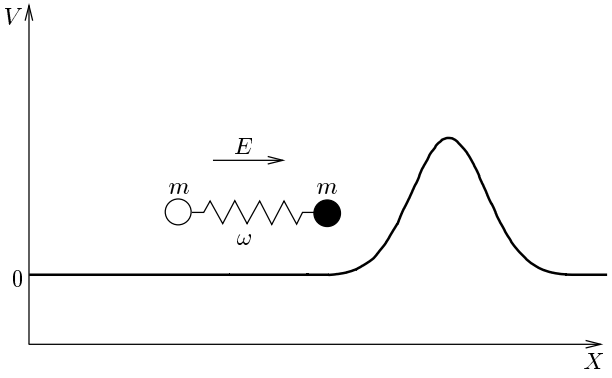

Fig. 1. An oscillator hitting a potential barrier, with only the «dark» particle interacting with the barrier

between the oscillator levels is much smaller than the barrier height V_0. The Hamiltonian of the model is

$$H = \frac{p_1^2}{2m} + \frac{p_2^2}{2m} + \frac{m\omega^2}{4}(x_1 - x_2)^2 + \\ + V_0 \exp\left(-\frac{x_1^2}{2\sigma^2}\right), \quad (1)$$

where the conditions on the oscillator frequency and potential barrier are

$$\hbar\omega \ll V_0, \\ \sigma \gg \hbar/\sqrt{mV_0}. \quad (2)$$

Because the variables do not separate, this is certainly a nontrivial system.

We choose units with $\hbar = 1$, $m = 1$. It is also convenient to treat the frequency ω as a dimensionless parameter, such that all physical quantities are dimensionless. In our subsequent numerical study, we use the value $\omega = 0.5$, but keep the notation «ω» in formulas. The system is semiclassical, i.e., conditions (2) are satisfied, if we choose $\sigma = 1/\sqrt{2\lambda}$ and $V_0 = 1/\lambda$, where λ is a small parameter. At the classical level, this parameter is irrelevant: after rescaling the variables[2)] as

$$x_1 \to x_1/\sqrt{\lambda}, \quad x_2 \to x_2/\sqrt{\lambda},$$

the small parameter enters only through the overall multiplicative factor $1/\lambda$ in the Hamiltonian. Therefore, the semiclassical technique can be developed as an asymptotic expansion in λ.

The properties of the system are made clearer by replacing the variables x_1 and x_2 with the center-of-mass coordinate

[2)] To keep the notation simple, we use the same symbols x_1, x_2 for the rescaled variables.

$$X \equiv \frac{x_1 + x_2}{\sqrt{2}}$$

and the relative oscillator coordinate

$$y \equiv \frac{x_1 - x_2}{\sqrt{2}}.$$

In terms of these variables, the Hamiltonian becomes

$$H = \frac{p_X^2}{2} + \frac{p_y^2}{2} + \frac{\omega^2}{2} y^2 + \frac{1}{\lambda} \exp\left(-\frac{\lambda (X+y)^2}{2}\right). \quad (3)$$

The interaction potential

$$U_{int} \equiv \frac{1}{\lambda} \exp\left(-\frac{\lambda (X+y)^2}{2}\right)$$

vanishes in the asymptotic regions $X \to \pm\infty$ and describes a potential barrier between these regions. At $X \to \pm\infty$, Hamiltonian (3) corresponds to an oscillator of the frequency ω moving along the center-of-mass coordinate X. The oscillator asymptotic state is characterized by its excitation number N and total energy

$$E = \frac{p_X^2}{2} + \omega\left(N + \frac{1}{2}\right).$$

We are interested in the transmissions through the potential barrier of the oscillator with given initial values of E and N.

2.2. T/θ boundary value problem

The probability of tunneling from a state with a fixed initial energy E and oscillator excitation number N from the asymptotic region $X \to -\infty$ to any state in the other asymptotic region $X \to +\infty$ is given by

$$\mathcal{T}(E,N) = \\ = \lim_{t_f - t_i \to \infty} \sum_f \left| \langle f | \exp\left(-i\hat{H}(t_f - t_i)\right) | E, N \rangle \right|^2, \quad (4)$$

where it is implicit that the initial and final states have support only well outside the range of the potential, with $X < 0$ and $X > 0$, respectively. Semiclassical methods are applicable if the initial energy and excitation number are parametrically large,

$$E = \tilde{E}/\lambda, \quad N = \tilde{N}/\lambda,$$

where $\tilde{E}$ and $\tilde{N}$ are kept constant as $\lambda \to 0$. The transition probability has the exponential form

$$\mathcal{T} = D \exp\left(-\frac{1}{\lambda} F(\tilde{E},\ \tilde{N})\right), \quad (5)$$

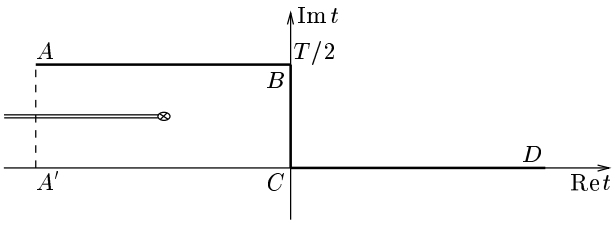

Fig. 2. Contour in the complex time plane

where D is a pre-exponential factor, which is not considered in this paper. Our purpose is to calculate the leading semiclassical exponent $F(\tilde{E},\tilde{N})$. The exponent for tunneling from the oscillator ground state is obtained in [11–13, 32] by taking the limit $\tilde{N} \to 0$ in $F(\tilde{E},\tilde{N})$.

In what follows, we rescale the variables as

$$X \to X/\sqrt{\lambda}, \quad y \to y/\sqrt{\lambda}$$

and omit the tilde over the rescaled quantities $\tilde{E}$ and $\tilde{N}$.

The exponent $F(E,N)$ is related to a complex trajectory that satisfies a certain complexified classical boundary value problem. We present the derivation of this problem in Appendix A. The outcome is as follows. There are two Lagrange multipliers T and θ, which are related to the parameters E and N characterizing the incoming state. The boundary value problem is conveniently formulated on the contour $ABCD$ in the complex time plane (see Fig. 2), with the imaginary part of the initial time equal to $T/2$. The coordinates $X(t)$ and $y(t)$ must satisfy the complexified equations of motion in the interior points of the contour, and must be real in the asymptotic future (region D):

$$\frac{\delta S}{\delta X(t)} = \frac{\delta S}{\delta y(t)} = 0, \quad (6a)$$

$$\begin{matrix} \operatorname{Im} y(t) \to 0, \\ \operatorname{Im} X(t) \to 0, \end{matrix} \quad \text{as } t \to +\infty. \quad (6b)$$

In the asymptotic past (region A of the contour, where $t = t' + iT/2$, t' is real negative), the interaction potential U_{int} can be neglected and the oscillator decouples,

$$y = \frac{1}{\sqrt{2\omega}} \left(u \exp(-i\omega t') + v \exp(i\omega t')\right).$$

The boundary conditions in the asymptotic past, $t' \to -\infty$, are that the center-of-mass coordinate X must be real, while the complex amplitudes of the decoupled oscillator must be linearly related,

$$\begin{matrix} \operatorname{Im} X \to 0, \\ v \to e^{\theta} u^*, \end{matrix} \quad \text{as } t' \to -\infty. \quad (6c)$$

Boundary conditions (6b) and (6c) in fact make eight real conditions (because, e.g., $\mathrm{Im}\, X(t') \to 0$ implies that both $\mathrm{Im}\, X$ and $\mathrm{Im}\, \dot{X}$ tend to zero), and completely determine the solution, up to the time translation invariance (see the discussion in Appendix A).

It is shown in Appendix A that a solution of this boundary value problem is an extremum of the functional

$$F[X, y; X^*, y^*; T, \theta] = -iS[X, y] + iS[X^*, y^*] - \\ - ET - N\theta + \text{Boundary Terms}. \quad (7)$$

The value of this functional at the extremum gives the exponent for the transition probability (up to the large overall factor $1/\lambda$, see Eq. (5)),

$$F(E,\ N) = 2\,\mathrm{Im}\, S_0(T,\ \theta) - ET - N\theta, \quad (8)$$

where S_0 is the action of the solution, integrated by parts,

$$S_0 = \int dt \left(-\frac{1}{2} X \frac{d^2 X}{dt^2} - \right. \\ \left. - \frac{1}{2} y \frac{d^2 y}{dt^2} - \frac{1}{2}\omega^2 y^2 - U_{int}(X, y) \right). \quad (9)$$

Here, the integration runs along the contour $ABCD$. The values of the Lagrange multipliers T and θ are related to the energy and excitation number as

$$E(T, \theta) = \frac{\partial}{\partial T} 2\,\mathrm{Im}\, S_0(T, \theta), \quad (10)$$

$$N(T, \theta) = \frac{\partial}{\partial \theta} 2\,\mathrm{Im}\, S_0(T, \theta). \quad (11)$$

Using Eq. (8), it is also straightforward to verify the inverse Legendre transformation formulas

$$T(E,\ N) = -\frac{\partial}{\partial E} F(E,\ N), \quad (12)$$

$$\theta(E,\ N) = -\frac{\partial}{\partial N} F(E,\ N). \quad (13)$$

It can also be verified that the right-hand side of Eq. (10) coincides with the energy of the classical solution and the right-hand side of Eq. (11) is equal to the classical counterpart of the occupation number,

$$E = \frac{\dot{X}^2}{2} + \omega N, \quad N = uv. \quad (14)$$

Therefore, we can either seek the values of T and θ that correspond to given E and N, or, following a computationally simpler procedure, solve the boundary value problem (6) for given T and θ and then find the corresponding values of E and N from Eq. (14). We note that initial conditions (6c) complemented by Eqs. (14) are equivalent to the initial conditions in Refs. [3–5], the latter being expressed in terms of action–angle variables. The boundary conditions in the asymptotic future, Eq. (6b), are different from those in Refs. [3–5], because we consider inclusive, rather than fixed, final state.

We now discuss some subtle points of boundary value problem (6). First, we note that the asymptotic reality condition in (6b) does not always coincide with the reality condition at finite time. Of course, if the solution approaches the asymptotic region $X \to +\infty$ on the part CD of the contour, asymptotic reality condition (6b) implies that the solution is real at any finite positive t. Indeed, the oscillator decouples as $X \to +\infty$, and therefore condition (6b) means that its phase and amplitude, as well as $X(t)$, are real as $t \to +\infty$. Due to the equations of motion, $X(t)$ and $y(t)$ are real on the entire CD part of the contour. This situation corresponds to the transition directly to the asymptotic region $X \to +\infty$. However, the situation can be drastically different if the solution on the final part of the time contour remains in the interaction region. For example, we can imagine that the solution approaches the saddle point of the potential $X = 0$, $y = 0$ as $t \to +\infty$. Because one of the perturbations around this point is unstable, there may exist solutions that approach this point exponentially along the unstable direction, i.e.,

$$X(t),\ y(t) \propto \exp(-\mathrm{const} \cdot t)$$

with possibly complex prefactors. In this case, the solution may be complex at any finite time, and become real only asymptotically, as $t \to +\infty$. Such a solution corresponds to tunneling to the saddle point of the barrier, after which the system rolls down classically towards $X \to +\infty$ (with probability of the order of 1, inessential for the tunneling exponent F). We see in Sec. 3.1 that the situation of this sort indeed occurs for some values of the energy and excitation number.

Second, because the interaction potential disappears at large negative time (in the asymptotic region $X \to -\infty$), it is straightforward to continue the asymptotic form of the solution to the real time axis. For solutions satisfying (6c), this gives

$$y(t) = \frac{1}{\sqrt{2\omega}} \left(u \exp\left(-\frac{\omega T}{2}\right) \exp(-i\omega t) + \right. \\ \left. + u^* \exp\left(\theta + \frac{\omega T}{2}\right) \exp(i\omega t) \right),$$

$$\mathrm{Im}\, X(t) = -\frac{T}{2} p_X$$

at large negative time. We see that the dynamical coordinates on the negative side of the real time axis are generally complex. For solutions approaching the asymptotic region $X \to +\infty$ as $t \to +\infty$ (such that X and y are exactly real at finite $t > 0$), this means that there should exist a branch point in the complex time plane: the contour $A'ABC$ in Fig. 2 winds around this point and cannot be deformed to the real time axis. This argument does not work for solutions ending in the interaction region as $t \to +\infty$, and hence branch points between the AB part of the contour and the real time axis may be absent. We see in Sec. 3.1 that this is indeed the case in our model in a certain range of E and N.

2.3. Over-barrier transitions: the region of classically allowed transitions and its boundary $E_0(N)$

Before studying the exponentially suppressed transitions, we consider the classically allowed ones. For this, we study the classical evolution (real time, real-valued coordinates) such that the system is initially located at large negative X and moves with a positive center-of-mass velocity towards the asymptotic region $X \to +\infty$. The classical dynamics of the system is specified by four initial parameters. One of them (e.g., the initial center-of-mass coordinate) fixes the invariance under time translations, while the other three are the total energy E, the initial excitation number of the y-oscillator, defined in classical theory as $N \equiv E_{osc}/\omega$, and the initial oscillator phase φ_i.

Any initial quantum state of our system can be fully determined by the energy E and the initial oscillator excitation number N; we can represent each state by a point in the EN plane. There is, however, one additional classically relevant initial parameter, the oscillator phase φ_i. An initial state (E, N) leads to unsuppressed transmission if the corresponding classical over-barrier transitions[3)] are possible for some value(s) of φ_i. These states form some region in the EN plane, which is to be found in this section.

For given N, at sufficiently large E, the system can certainly evolve to the other side of the barrier. On the other hand, if E is smaller than the barrier height, the system definitely undergoes reflection. Thus, there exists some boundary energy $E_0(N)$ such that classical transitions are possible for $E > E_0(N)$, while for $E < E_0(N)$ they do not occur for any initial phase φ_i. The line $E_0(N)$ represents the boundary of the region of classically allowed transitions. We have calculated $E_0(N)$ numerically: the result[4)] is shown in Fig. 3.

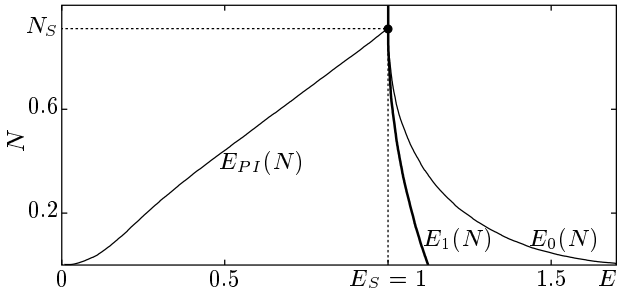

Fig. 3. The boundary $E_0(N)$ of the region of classically allowed transitions, the bifurcation line $E_1(N)$, and the line of the periodic instantons $E_{PI}(N)$

An important point of the boundary $E_0(N)$ corresponds to the static unstable classical solution $X(t) = y(t) = 0$. In the field theory context, such a solution is called «sphaleron» [33], and we keep this terminology in what follows. This solution is the saddle point of the potential

$$U(X, y) \equiv \omega^2 y^2/2 + U_{int}(X, y)$$

and has exactly one unstable direction, the negative mode (see Fig. 4). The sphaleron energy $E_S = U(0, 0) = 1$ determines the minimum value of the function $E_0(N)$. Indeed, classical over-barrier transitions with $E < E_S$ are impossible, but the over-barrier solution with a slightly higher energy can be obtained as follows: a momentum along the negative mode is added at the point $X = y = 0$, «pushing» the system towards $X \to +\infty$. Continuing this solution backwards in time shows that the system tends to $X \to -\infty$ for large negative time and has a certain oscillator excitation number. Solutions with the energy closer to the sphaleron energy correspond to a smaller «push» and thus spend longer time near the sphaleron. In the limiting case where the energy is equal to E_S, the solution spends an infinite time in the vicinity of the sphaleron. This limiting case has a definite initial excitation number N_S, such that $E_0(N_S) = E_S$ (see Fig. 3). The

[3)] We note that the corresponding classical solutions obey boundary conditions (6b) and (6c) with $T = \theta = 0$, i.e., they are solutions to boundary value problem (6).

[4)] We note that the boundary $E_0(N)$ of the region of classically allowed transitions can be extended to $N > N_S$. Because $E = E_S$ is the absolute minimum of the energy of classically allowed transitions, the function $E_0(N)$ grows with N at $N > N_S$. In fact, it tends to the asymptotics $E_0^{as} = \omega N$ as $N \to +\infty$. In what follows, we are not interested in transitions with $N > N_S$, and therefore this part of the boundary $E_0(N)$ is not shown in Fig. 3.

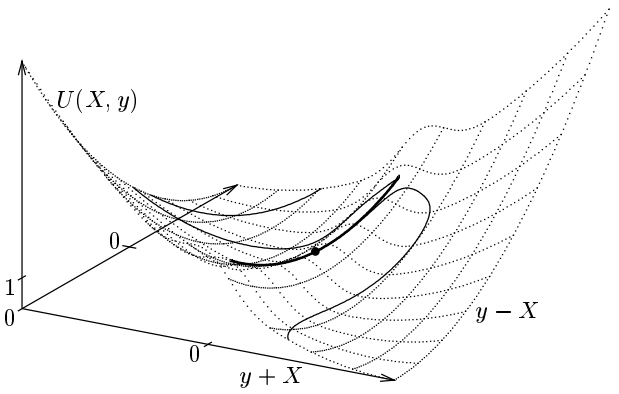

Fig. 4. The potential (dotted lines) in the vicinity of the sphaleron ($X = 0,\ y = 0$) (marked by the point), the excited sphaleron (thick line) corresponding to the point $(E, N) = (1.985, 3.72)$ at the boundary of the region of classically allowed transitions, and the trajectory of the solution that is close to this excited sphaleron (thin line). The asymptotic regions $X \to \pm\infty$ are along the diagonal

value of N_S is unique because there is exactly one negative direction of the potential in the vicinity of the sphaleron.

In complete analogy to the features of the over-barrier classical solutions near the sphaleron point (E_S, N_S), we expect that as the values of E and N approach any other boundary point ($E_0(N)$, N), the corresponding over-barrier solutions spend more and more time in the interaction region, where $U_{int} \neq 0$. This follows from a continuity argument. Namely, we first fix the initial and final times, t_i and t_f. If within this time interval a solution with the energy E_1 evolves to the other side of the barrier and a solution with the energy E_2 and the same oscillator excitation number is reflected, there exists an intermediate energy at which the solution ends up at $t = t_f$ in the interaction region. Taking the limit as $t_f \to +\infty$ and $E_1 - E_2 \to 0$, we obtain a point at the boundary $E_0(N)$ and a solution tending asymptotically to some unstable time-dependent solution that spends infinite time in the interaction region. We call the latter solution the excited sphaleron; it describes some (in general, nonlinear) oscillations above the sphaleron along the stable direction in the coordinate space. Therefore, every point of the boundary ($E_0(N)$, N) corresponds to some excited sphaleron. In the phase space, solutions tending asymptotically to the excited sphalerons form a surface (separatrix) that separates regions of qualitatively different classical motions of the system.

In Fig. 4, we display a solution, found numerically in our model, that tends to an excited sphaleron. We see that the trajectory of the excited sphaleron is, roughly speaking, orthogonal to the unstable direction at the saddle point ($X = 0, y = 0$).

2.4. Suppressed transitions: bifurcation line $E_1(N)$

We now turn to classically forbidden transitions and consider the boundary value problem in Eq. (6). It is relatively straightforward to obtain solutions for $\theta = 0$ numerically. In this case, boundary conditions (6b) and (6c) take the form of reality conditions in the asymptotic future and past. It can be shown [34] that the physically relevant solutions with $\theta = 0$ are real on the entire contour $ABCD$ in Fig. 2 and describe nonlinear oscillations in the upside-down potential on the Euclidean part BC of the contour. The period of the oscillations is equal to T, and hence the points B and C are two different turning points where $\dot{X} = \dot{y} = 0$. These real Euclidean solutions are called periodic instantons. A practical technique for obtaining these solutions numerically on the Euclidean part BC consists in minimizing the Euclidean action (for example, with the method of conjugate gradients, see Ref. [11, 12] for the details). The solutions on the entire contour are then obtained by solving the Cauchy problem numerically, forward in time along the line CD and backward in time along the line BA. From the solution in the asymptotic past (region A), we then calculate its energy and excitation number (14). The solutions of this Cauchy problem are obviously real, and hence boundary conditions (6b) and (6c) are indeed satisfied for $\theta = 0$. It is worth noting that solutions with $\theta = 0$ are similar to the ones in quantum mechanics of one degree of freedom. The line of periodic instantons in the EN plane in our model is shown in Fig. 3.

Once the solutions with $\theta = 0$ are found, it is natural to try to cover the entire region of classically forbidden transitions in the EN plane with a deformation procedure, by moving in small steps in θ and T. The solution of the boundary value problem with ($T + \Delta T$, $\theta + \Delta\theta$) may be obtained numerically, by applying an iteration technique, with the known solution at (T, θ) serving as the initial approximation[5)]. If the solutions end up in the correct asymptotic region at each step, i.e., $X \to +\infty$ on part D of the contour, the solutions obtained by this procedure of small deformations are physically relevant. But the method of small defor-

[5)] In practice, the Newton–Raphson method is particularly convenient (see Refs. [11, 12, 14, 15]).

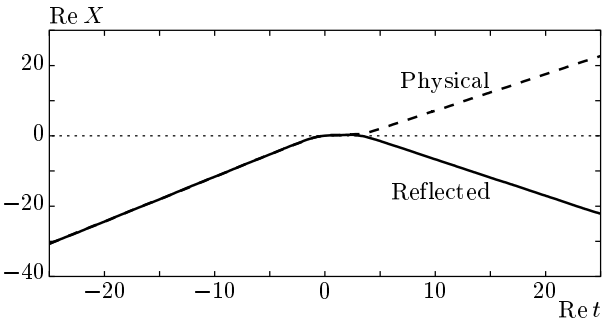

Fig. 5. The dependence of the tunneling coordinate X on time for two solutions with nearly the same energy and initial excitation number. The physical solution tunnels to the asymptotic region $X \to +\infty$, while the unphysical one is reflected to $X \to -\infty$. The physical solution has $E = 1.028$, $N = 0.44$, while the unphysical one has $E = 1.034$, $N = 0.44$. These two solutions are close to the point on the bifurcation line $E_1(N = 0.44) = 1.031$

mations fails to produce relevant solution if there are bifurcation points in the EN plane, where the physical branch of solutions merges to an unphysical branch. Because there are unphysical solutions close to physical ones in the vicinity of bifurcation points, the procedure of small deformations cannot be used near these points.

We have found numerically that in our model, the method of small deformations produces correct solutions of the T/θ boundary value problem in a large region of the EN plane where $E < E_1(N)$. However, at sufficiently high energy $E > E_1(N)$, where $E_1(N) \gtrsim E_S$, the deformation procedure generates solutions that bounce back from the barrier (see Fig. 5), i.e., have a wrong «topology». This occurs deep inside the region of classically forbidden transitions, where the suppression is large, and one naively expects the semiclassical technique to work well. Clearly, solutions with a wrong topology do not describe the tunneling transitions of interest. Therefore, if the semiclassical method is applicable in the region $E_1(N) < E < E_0(N)$ at all, there exists another, physical branch of solutions. In that case, the line $E_1(N)$ is the bifurcation line where the physical solutions «meet» the ones with a wrong «topology». Walking in small steps in θ and T is useless in the vicinity of this bifurcation line, and a special trick is required to find the relevant solutions beyond that line. The bifurcation line $E_1(N)$ for our quantum mechanical problem of two degrees of freedom is shown in Fig. 3.

The loss of topology beyond a certain bifurcation line in the EN plane is by no means a property of our model only. This phenomenon has been observed in field theory models, in the context of both induced false vacuum decay [14] and baryon-number violating transitions in gauge theory [15] (in field theory models, the parameter N is the number of incoming particles). In all cases, the loss of topology prevented one from computing the semiclassical exponent for the transition probability in the interesting region of relatively high energies.

Returning to quantum mechanics of two degrees of freedom, we point out that the properties of tunneling solutions with different energies approaching the bifurcation line $E_1(N)$ from the left of the EN plane are in some sense similar to the properties of tunneling solutions in one-dimensional quantum mechanics whose energy is close to the barrier height, see Appendix C. Again by continuity, these solutions of our two-dimensional model spend a long time in the interaction region; this time tends to infinity on the line $E_1(N)$. Hence, at any point of this line, there is a solution that starts in the asymptotic region left of the barrier and ends up on an excited sphaleron. Such behavior is indeed possible because of the existence of an unstable direction near the (excited) sphaleron, even for complex initial data. In the next section, we suggest a trick to deal with this situation — this is our regularization technique.

3. REGULARIZATION TECHNIQUE

In this section, we develop our regularization technique and find the physically relevant solutions between the lines $E_1(N)$ and $E_0(N)$. We see that all solutions from the new branch (and not only on the lines $E_0(N)$ and $E_1(N)$) correspond to tunneling onto the excited sphaleron («tunneling on top of the barrier»). These solutions would be very difficult, if at all possible, to obtain directly, by numerically solving the nonregularized classical boundary value problem (6): they are complex at finite times and become real only asymptotically as $t \to +\infty$, whereas numerical methods require working with finite time intervals.

As an additional advantage, our regularization technique allows obtaining a family of over-barrier solutions that covers all the region of the initial data corresponding to classicaly allowed transitions, including its boundary. This is of interest in models with a large number of the degrees of freedom and in field theory, where finding the boundary $E_0(N)$ by direct methods is difficult (see e.g., Ref. [35] for a discussion of this point).

3.1. Regularized problem: classically forbidden transitions

The main idea of our method is to regularize the equations of motion by adding a term proportional to a small parameter ϵ such that configurations staying near the sphaleron for an infinite time no longer exist among the solutions of the T/θ boundary value problem. After performing the regularization, we explore all the region of classically forbidden transitions without crossing the bifurcation line. Taking the limit $\epsilon \to 0$, we then reconstruct the correct values of F, E, and N.

In formulating the regularization technique, it is more convenient to work with the functional $F[X, y; X^*, y^*; T, \theta]$, Eq. (7), itself rather than with the equations of motion. We prevent F from being extremized by configurations approaching the excited sphalerons asymptotically. To achieve this, we add a new term of the form $2\epsilon T_{int}$ to the original functional (7), where T_{int} estimates the time that the solution «spends» in the interaction region. The regularization parameter ϵ is the smallest one in the problem, and hence any regular extremum of the functional F (the solution that spends finite time in the region $U_{int} \neq 0$) changes only slightly after the regularization. At the same time, the excited sphaleron configuration has $T_{int} = \infty$, which leads to the infinite value of the regularized functional

$$F_\epsilon \equiv F + 2\epsilon T_{int}.$$

Hence, the excited sphalerons are not stationary points of the regularized functional.

For the problem under consideration, $U_{int} \sim 1$ in the interaction region, and T_{int} can be defined as

$$T_{int} = \frac{1}{2}\left[\int dt\, U_{int}(X, y) + \int dt\, U_{int}(X^*, y^*)\right]. \quad (15)$$

We note that T_{int} is real and that the regularization is equivalent to the multiplication of the interaction potential with a complex factor,

$$U_{int} \to (1 - i\epsilon)U_{int} = e^{-i\epsilon}U_{int} + O(\epsilon^2). \quad (16)$$

This results in the corresponding change of the classical equations of motion, while boundary conditions (6b) and (6c) remain unaltered.

We still have to understand whether solutions with $\epsilon \neq 0$ exist at all. The reason for the existence of such solutions is as follows. We consider a well-defined (for $\epsilon > 0$) matrix element

$$\mathcal{T}_\epsilon = \lim_{t_f - t_i \to \infty} \sum_f \left| \langle f | \exp\left[(-i\hat{H} - \epsilon U_{int})(t_f - t_i)\right] \times \right.$$
$$\left. \times\ |E, N\rangle \right|^2,$$

where, as before, $|E,\ N\rangle$ denotes the incoming state with given energy and oscillator excitation number. The quantity $\mathcal{T}_\epsilon$ has a well-defined limit as $\epsilon \to 0$, equal to tunneling probability (4). Because the saddle point of the regularized functional F_ϵ gives the semiclassical exponent for the quantity $\mathcal{T}_\epsilon$, we expect that such a saddle point indeed exists.

Therefore, the regularized T/θ boundary value problem is expected to have solutions necessarily spending finite time in the interaction region. By continuity, these solutions do not experience reflection from the barrier if the procedure of small deformations starting from solutions with the correct «topology» is used. The line $E_1(N)$ is no longer a bifurcation line of the regularized system, and the procedure of small deformations therefore enables us to cover the entire region of classically forbidden transitions. The semiclassical suppression factor of the original problem is recovered in the limit $\epsilon \to 0$.

It is worth noting that the interaction time is Legendre conjugate to ϵ,

$$T_{int} = \frac{1}{2}\frac{\partial}{\partial \epsilon} F_\epsilon(E, N, \epsilon). \quad (17)$$

This equation can be used as a check of numerical calculations.

We implemented the regularization procedure numerically. To solve the boundary value problem, we use the computational methods described in Ref. [11, 12]. To obtain the semiclassical tunneling exponent in the region between the bifurcation line $E_1(N)$ and the boundary of the region of classically allowed transitions $E_0(N)$, we began with a solution to the nonregularized problem deep in the «forbidden» region of the initial data (i.e., at $E < E_1(N)$). We then increased the value of ϵ from zero to a certain small positive number, keeping T and θ fixed. We next changed T and θ in small steps, keeping ϵ finite, and found solutions of the regularized problem in the region $E_1(N) < E < E_0(N)$. These solutions had the correct «topology», i.e., they indeed ended up in the asymptotic region $X \to +\infty$. Finally, we lowered ϵ and extrapolated F, E, and N to the limit $\epsilon \to 0$.

We now consider the solutions in the region $E_1(N) < E < E_0(N)$, which we obtain in the limit $\epsilon \to 0$, more carefully. They belong to a new branch, and may therefore exhibit new physical properties. Indeed, we found that as the value of ϵ

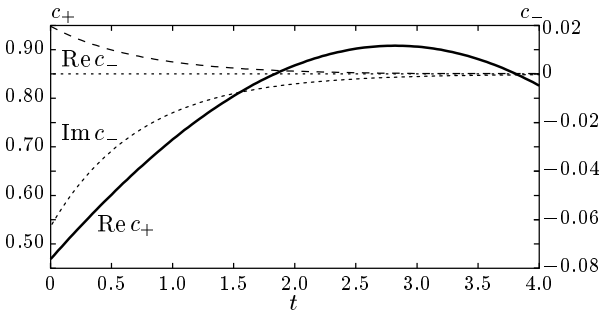

Fig. 6. Large-time behavior of a solution with $\epsilon = 0$ at $(E = 1.05,\ N = 0.43)$. The coordinates X and y are decomposed in the basis of the eigenmodes near the sphaleron. We note that $\mathrm{Im}\, c_+ = 0$

decreases to zero, the solution at any point (E, N) with $E_1(N) < E < E_0(N)$ spends more and more time in the interaction region. The limiting solution corresponding to $\epsilon = 0$ has infinite interaction time: in other words, as $t \to +\infty$, it tends to one of the excited sphalerons. The resulting physical picture is that at a sufficiently large energy (i.e., at $E > E_1(N)$), the system prefers to tunnel exactly onto an unstable classical solution, excited sphaleron, that oscillates about the top of the potential barrier. To demonstrate this, we have plotted in Fig. 6 the solution $\mathbf{x}(t) \equiv (X(t), y(t))$ at large times, after taking the limit $\epsilon \to 0$ numerically. To understand this figure, we recall that the potential near the sphaleron point $X = y = 0$ has one positive mode and one negative mode. Namely, introducing new coordinates c_+, c_- as

$$X = \cos\alpha\ c_+ + \sin\alpha\ c_-,$$

$$y = -\sin\alpha\ c_+ + \cos\alpha\ c_-,$$

$$\mathrm{ctg}\, 2\alpha = -\frac{\omega^2}{2},$$

we write, in the vicinity of the sphaleron,

$$H = 1 + \frac{p_+^2}{2} + \frac{p_-^2}{2} + \frac{\omega_+^2}{2}c_+^2 - \frac{\omega_-^2}{2}c_-^2,$$

where

$$\omega_\pm^2 = \pm\left(-1 + \frac{\omega^2}{2}\right) + \sqrt{1 + \frac{\omega^4}{4}} > 0.$$

Because the solutions of the T/θ boundary value problem are complex, the coordinates c_+ and c_- are also complex. In Fig. 6, we show real and imaginary parts of c_+ and c_- at a large real time t (part CD of the contour). We see that while $\mathrm{Re}\, c_+$ oscillates, the unstable coordinate c_- asymptotically approaches the sphaleron value: $c_- \to 0$ as $t \to +\infty$. The imaginary part of c_- is nonzero at any finite time. This is the reason for the failure of straightforward numerical methods in the region $E > E_1(N)$: the solutions from the physical branch do not satisfy the reality conditions at any large but finite final time. We have pointed out in Sec. 2.2 that this can happen only if the solution ends up near the sphaleron, which has a negative mode. This is precisely what happens: for $\epsilon = 0$ at asymptotically large t, our solutions are real and oscillate near the sphaleron, remaining in the interacton region.

3.2. Regularization technique versus exact quantum mechanical solution

Quantum mechanics of two degrees of freedom is a convenient testing ground for checking the semiclassical methods and, in particular, our regularization technique. We have found solutions of the full stationary Schrödinger equation and exact tunneling probability $\mathcal{T}$ by applying the numerical technique in Refs. [11, 12]. Our numerical calculations were performed for several small values of the semiclassical parameter λ, namely, for $\lambda = 0.01$–0.1. Transitions through the barrier for these values of the semiclassical parameter are well suppressed. In particular, for $\lambda = 0.02$, the tunneling probability $\mathcal{T}$ is of the order e^{-14}. To check the semiclassical result with better precision, we have calculated the exact suppression exponent

$$F_{QM}(\lambda) \equiv -\lambda \log \mathcal{T}$$

(cf. (5)) for $\lambda = 0.09, 0.05, 0.03, 0.02$ and extrapolated F_{QM} to $\lambda = 0$ by polynomials of the third and fourth degree. The extrapolation results are independent of the degree (3 or 4) of polynomials with the precision 1 %. The extrapolated suppression exponent $F_{QM}(0)$ corresponds to infinite suppression and must exactly coincide (up to numerical errors) with the correct semiclassical result.

We performed this check in the region $E > E_S = 1$, which is most interesting for our purposes. The results of the full quantum mechanical calculation of the suppression exponent F_{QM} in the limit $\lambda \to 0$ are represented by points in Fig. 7. The lines in that figure represent the values of the semiclassical exponent $F(E, N)$ for constant N, which we obtain in the limit $\epsilon \to 0$ of the regularization procedure. In practice, instead of taking the limit $\epsilon \to 0$, we calculate the regularized functional

$$F_\epsilon(E, N) = F(E, N) + O(\epsilon)$$

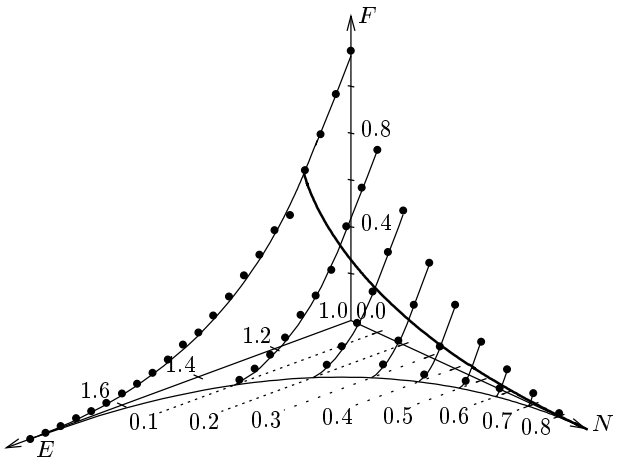

Fig. 7. The tunneling exponent $F(E,N)$ in the region $E > E_S = 1$. The lines show the semiclassical results and the dots represent exact ones, obtained by solving the Schrödinger equation. The lines across the plot are the boundary of the region of classically allowed transitions $E_0(N)$ and the bifurcation line $E_1(N)$

for sufficiently small ϵ. We used the value $\epsilon = 10^{-6}$, and the value of the suppression exponent was then found with the precision of the order 10^{-5}. We see that in the entire region of classically forbidden transitions (including the region $E > E_1(N)$), the semiclassical result for F coincides with the exact one.

3.3. Classically allowed transitions

We now show that our regularization procedure allows obtaining a subset of classical over-barrier solutions existing at sufficiently high energies. This subset is interesting because it extends to the boundary of the region of classically allowed transitions, $E = E_0(N)$. In principle, finding this boundary is purely a problem of classical mechanics; indeed, in the mechanics of two degrees of freedom, this boundary can be found numerically by solving the Cauchy problem for given E and N and all possible oscillator phases, see Sec. 2.3. But if the number of the degrees of freedom is much larger, this classical problem becomes quite complicated, because a high-dimensional space of Cauchy data has to be spanned. As an example, a stochastic Monte Carlo technique was developed in Ref. [35] to deal with this problem in the field theory context. The approach below is an alternative to the Cauchy methods.

We first recall that all classical over-barrier solutions with given energy and excitation number satisfy the T/θ boundary value problem with $T = 0$, $\theta = 0$. We cannot reach the «allowed» region of the EN plane without regularization, because we have to cross the line $E_0(N)$ corresponding to the excited sphaleron configurations in the final state. But the excited sphalerons no longer exist among the solutions of the regularized boundary value problem at any finite value of ϵ. This suggests that the regularization allows entering the region of classically allowed transitions and, after taking an appropriate limit, obtaining classical solutions with finite values of E and N.

By definition, the classically allowed transitions have $F = 0$. We therefore expect that in the «allowed» region of the initial data, the regularized problem has the property that

$$F_\epsilon(E,N) = \epsilon f(E,N) + O(\epsilon^2).$$

In view of the inverse Legendre formulas (12) and (13), the values of T and θ must be of the order of ϵ,

$$T = \epsilon\tau(E,N), \quad \theta = \epsilon\vartheta(E,N),$$

where the quantities τ and ϑ are related to the initial energy and excitation number (see Eqs. (12), (13)) as

$$\tau = -\lim_{\epsilon\to 0} \frac{\partial}{\partial E}\frac{F_\epsilon}{\epsilon} = -\frac{1}{2}\frac{\partial}{\partial E} T_{int}(E,N), \qquad (18)$$

$$\vartheta = -\lim_{\epsilon\to 0} \frac{\partial}{\partial N}\frac{F_\epsilon}{\epsilon} = -\frac{1}{2}\frac{\partial}{\partial N} T_{int}(E,N), \qquad (19)$$

where we have used Eq. (17). We thus expect that the region of classically allowed transitions can be invaded by taking a fairly sophisticated limit $\epsilon \to 0$ with $\tau \equiv T/\epsilon = \text{const}$, $\vartheta \equiv \theta/\epsilon = \text{const}$. For the allowed transitions, the parameters τ and ϑ are analogous to T and θ.

Solving the regularized T/θ boundary value problem allows constructing a single solution for given E and N. On the other hand, for $\epsilon = 0$, there are more classical over-barrier solutions: they form a continuous family labeled by the initial oscillator phase. Thus, taking the limit $\epsilon \to 0$ gives a subset of over-barrier solutions, which should therefore obey some additional constraint. It is almost obvious that this constraint is that the interaction time T_{int}, Eq. (15), is minimal. This is shown in Appendix B.

The subset of classical over-barrier solutions obtained in the $\epsilon \to 0$ limit of the regularized T/θ procedure extends to the boundary of the region of classically allowed transitions. We now consider what happens as this boundary is approached from the «classically allowed» side. At the boundary $E_0(N)$, the unregularized solutions tend to excited sphalerons, and the interaction time T_{int} is therefore infinite. This is consistent with (18) and (19) only if τ and ϑ become infinite at the

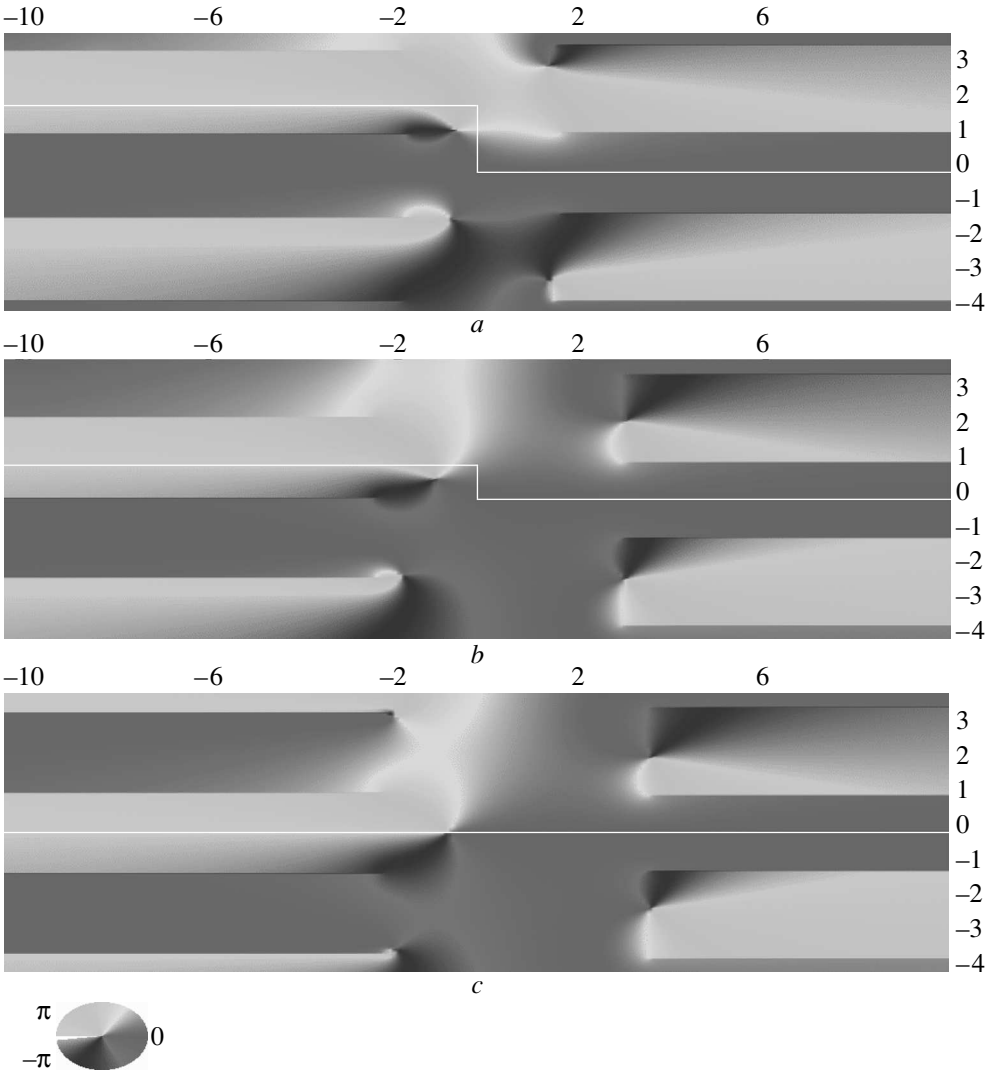

Fig. 8. The phase of the tunneling coordinate in the complex time plane at three points of the curve $\tau = 380$, $\vartheta = 130$. Figures a, b, and c correspond to $\epsilon = \epsilon_a = 0.01$, $\epsilon = \epsilon_b = 0.0048$, and $\epsilon = \epsilon_c = 0$ respectively. The asymptotics $X \to -\infty$ and $X \to +\infty$ correspond to $\arg X = \pi$ and 0. The contour in the time plane is plotted with the white line

boundary. Hence, to obtain a point of the boundary, we takes the further limit,

$$\big(E_0(N),\, N\big) = \lim_{\substack{\tau/\vartheta=\text{const} \\ \tau\to+\infty}} \big(E(\tau,\vartheta), N(\tau,\vartheta)\big).$$

Different values of τ/ϑ correspond to different points of the line $E_0(N)$. We thus find the boundary of the region of classically allowed transitions without initial-state simulation.

We have checked this procedure numerically. The limit $\epsilon \to 0$ exists indeed — the values of E and N tend to the point of the EN plane that corresponds to the classically allowed transition. The phase of the tunneling coordinate $X(t)$ in the complex time plane is shown in Fig. 8 for the three points (Figs. a, b, and c) of the curve $\tau \equiv T/\epsilon = 380$, $\vartheta \equiv \theta/\epsilon = 130$. Point a lies deep inside the tunneling region, $E_a < E_1(N_a)$, point c corresponds to the over-barrier solution with $T = 0$, $\theta = 0$, $\epsilon = 0$, and point b is in the middle of the curve. The branch points of the solution, the cuts, and the contour are clearly seen on these graphs[6)].

It is worth noting that the left branch points move down as T and θ approach zero. Solutions close enough

[6)] The phase of the tunneling coordinate changes by π around the branch point. The points where the phase of the tunneling coordinate changes by 2π correspond to zeroes of $X(t)$.

to the boundary $E_0(N)$ have the left branch point in the lower complex half-plane, see Fig. 8. Therefore, the corresponding contour can be continuously deformed to the real time axis. These solutions still satisfy the reality conditions asymptotically (see Fig. 6), but show nontrivial complex behavior at any finite time.

The regularized T/θ procedure allows approaching the boundary of the region of classically allowed transitions from both sides. The points at this boundary are obtained by taking the limits $T \to 0$, $T/\theta = \text{const}$ of the tunneling solutions and $\tau \to +\infty$, $\tau/\vartheta = \text{const}$ of the classically allowed ones. Because $\tau^* \equiv \tau/\vartheta = T/\theta$ by construction, the lines $\tau^* = \text{const}$ are continuous at the boundary $E_0(N)$, although may have discontinuity of the derivatives. The variable τ^* can be used to parameterize the curve $E_0(N)$.

4. CONCLUSIONS

We conclude that classical solutions describing transmissions of a bound system through a potential barrier with different values of the energy and the initial oscillator excitation number form three branches. These branches merge at bifurcation lines $E_0(N)$ and $E_1(N)$. Solutions from different branches describe physically different transition processes. Namely, solutions at low energies $E < E_1(N)$ describe the conventional potential-like tunneling. At $E > E_0(N)$, they correspond to unsuppressed over-barrier transitions. At intermediate energies, $E_1(N) < E < E_0(N)$, physically relevant solutions describe transitions on top of the barrier. This branch structure is shown in Fig. 9*a*, where the period $T = \partial F/\partial E$ obtained numerically for solutions from the different branches is plotted as a function of energy for $N = 0.1$.

We note that the qualitative structure of branches in the model with internal degrees of freedom is similar to the structure of branches in one-dimensional quantum mechanics (see Appendix C). The latter is shown in Fig. 9*b*. The features of solutions in both cases are similar, although the solutions ending up on top of the barrier are degenerate in energy in the one-dimensional case, and hence are not physically interesting.

In this paper, we introduced the regularization technique that allows smoothly connecting solutions in different branches. Its advantage is that it automatically chooses the physically relevant branch. This technique is particularly convenient in numerical studies: we have seen that it allows covering the whole interesting region of the parameter space. We applied this technique to baryon number violating processes in electroweak theory [16].

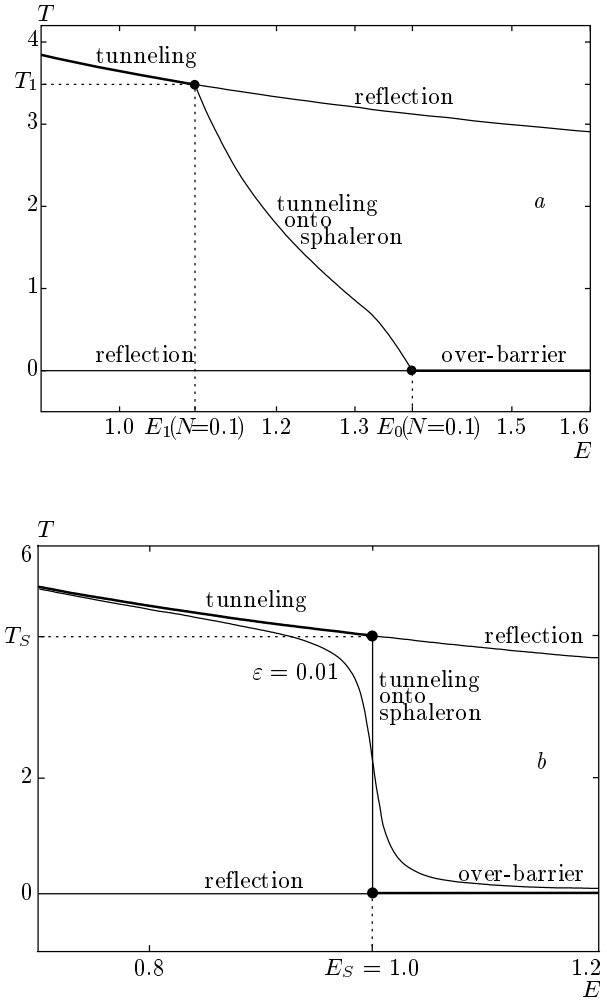

Fig. 9. The dependence of the parameter $T = -\partial F/\partial E$ on the energy for (*a*) the two-dimensional model with fixed $N = 0.1$ and (*b*) the one-dimensional model (see Appendix C). Different lines correspond to different branches of classical solutions of the T/θ boundary value problem. The branches labeled «reflection» end up on the wrong side of the barrier. Figure *b* also contains a line with nonzero ϵ

The authors are indebted to V. Rubakov and C. Rebbi for numerous valuable discussions and criticism, A. Kuznetsov, W. Miller, and S. Sibiryakov for helpful discussions, and S. Dubovsky, D. Gorbunov, A. Penin, and P. Tinyakov for stimulating interest. We wish to thank Boston University Center for Computational Science and Office of Information Technology for allocation of supercomputer time. This research was supported by the RFBR (grant № 02-02-17398), grant of the President of the Russian Federation № NS-2184.2003.2, U. S. Civilian

Research and Development Foundation for Independent States of FSU (CRDF) award RP1-2364-MO-02, and the DOE grant № US DE-FG02-91ER40676. F. B. is supported by the Swiss Science Foundation (grant № 7SUPJ062239).

APPENDIX A

T/θ boundary value problem

The semiclassical method for calculating the probability of tunneling from a state with a few parameters fixed was developed in [13–15, 32] in the context of field theory models and in [3–5, 11, 12] in quantum mechanics. Here, we outline the method adapted to our model of two degrees of freedom.

1. Path integral representation of the transition probability

We begin with the path integral representation for the probability of tunneling from the asymptotic region $X \to -\infty$ through a potential barrier. Let the incoming state $|E,\ N\rangle$ have fixed energy and oscillator excitation number, and have support only for $X \ll 0$, well outside the range of the potential barrier. The inclusive tunneling probability for states of this type is given by

$$\mathcal{T}(E,N) = \lim_{t_f - t_i \to \infty} \left\{ \int_0^{+\infty} dX_f \int_{-\infty}^{+\infty} dy_f \times \right.$$
$$\left. \times \left| \langle X_f, y_f | \exp(-i\hat{H}(t_f - t_i)) | E, N \rangle \right|^2 \right\}, \quad \text{(A.1)}$$

where $\hat{H}$ is the Hamiltonian operator. This probability can be reexpressed in terms of the transition amplitudes

$$\mathcal{A}_{fi} = \langle X_f,\ y_f | \exp(-i\hat{H}(t_f - t_i)) | X_i,\ y_i \rangle \quad \text{(A.2)}$$

and the initial-state matrix elements

$$\mathcal{B}_{ii'} = \langle X_i,\ y_i | E,\ N \rangle \langle E,\ N | X_i',\ y_i' \rangle \quad \text{(A.3)}$$

as

$$\mathcal{T}(E,\ N) = \lim_{t_f - t_i \to \infty} \left\{ \int_0^{+\infty} dX_f \int_{-\infty}^{0} dX_i\, dX_i' \times \right.$$
$$\left. \times \int_{-\infty}^{+\infty} dy_i\, dy_i'\, dy_f\ \mathcal{A}_{fi} \mathcal{A}^*_{i'f} \mathcal{B}_{ii'} \right\}. \quad \text{(A.4)}$$

The transition amplitude and its complex conjugate have the familiar path integral representation

$$\mathcal{A}_{fi} = \int [d\mathbf{x}] \Big|_{\substack{\mathbf{x}(t_i)=\mathbf{x}_i \\ \mathbf{x}(t_f)=\mathbf{x}_f}} \exp(iS[\mathbf{x}]),$$
$$\mathcal{A}^*_{i'f} = \int [d\mathbf{x}'] \Big|_{\substack{\mathbf{x}'(t_i)=\mathbf{x}_i' \\ \mathbf{x}'(t_f)=\mathbf{x}_f}} \exp(-iS[\mathbf{x}']), \quad \text{(A.5)}$$

where $\mathbf{x} = (X, y)$ and S is the action of the model. To obtain a similar representation for the initial-state matrix elements, we rewrite $\mathcal{B}_{ii'}$ as

$$\mathcal{B}_{ii'} = \langle X_i,\ y_i | \hat{P}_E \hat{P}_N | X_i',\ y_i' \rangle, \quad \text{(A.6)}$$

where $\hat{P}_N$ and $\hat{P}_E$ denote the projectors onto the respective states with the oscillator excitation number N and the total energy E. It is convenient to use the coherent state formalism for the y-oscillator and choose the momentum basis for the X-coordinate. In this representation, the kernel of the projector operator $\hat{P}_E \hat{P}_N$ becomes

$$\langle q,\ b | \hat{P}_E \hat{P}_N | p,\ a \rangle = \frac{1}{(2\pi)^2} \int d\xi\, d\eta \times$$
$$\times \exp\left(-iE\xi - iN\eta + \frac{i}{2} p^2 \xi + \exp(i\omega\xi + i\eta) \bar{b} a \right) \delta(q - p),$$

where $|p,\ a\rangle$ is the eigenstate with the respective eigenvalues p and a of the center-of-mass momentum $\hat{p}_X$ and the y-oscillator annihilation operator $\hat{a}$. It is straightforward to express this matrix element in the coordinate representation using the formulas

$$\langle y | a \rangle = \sqrt[4]{\frac{\omega}{\pi}} \exp\left(-\frac{1}{2} a^2 + \sqrt{2\omega} a y - \frac{1}{2} \omega y^2 \right),$$
$$\langle X | p \rangle = \frac{1}{\sqrt{2\pi}} \exp(ipX).$$

Evaluating the Gaussian integrals over a, b, p, and q, we obtain

$$\mathcal{B}_{ii'} = \int d\xi\ d\eta \exp\left\{ -iE\xi - iN\eta - \frac{i}{2} \frac{(X_i - X_i')^2}{\xi} + \right.$$
$$+ \frac{\omega}{1 - \exp(-2i\omega\xi - 2i\eta)} \times$$
$$\left. \times \left[\frac{y_i^2 + y_i'^2}{2} (1 + \exp(-2i\omega\xi - 2i\eta)) - \right. \right.$$
$$\left. \left. - 2 y_i y_i' \exp(-i\omega\xi - i\eta) \right] \right\}, \quad \text{(A.7)}$$

where we omit the pre-exponential factor depending on η and ξ. For the subsequent formulation of the boundary value problem, it is convenient to introduce the notation

$$T = -i\xi, \quad \theta = -i\eta.$$

Then, combining integral representations (A.7) and (A.5) and rescaling the coordinates, energy, and excitation number as $\mathbf{x} \to \mathbf{x}/\sqrt{\lambda}$, $E \to E/\lambda$, $N \to N/\lambda$, we finally obtain

$$\mathcal{T}(E,\ N) = \lim_{t_f - t_i \to \infty} \left\{ \int\limits_{-i\infty}^{+i\infty} dT\, d\theta \int [d\mathbf{x}\, d\mathbf{x}'] \times \right.$$
$$\left. \times \exp\left\{ -\frac{1}{\lambda} F[\mathbf{x},\ \mathbf{x}';\ T,\ \theta] \right\} \right\}, \quad \text{(A.8)}$$

where

$$F[\mathbf{x},\ \mathbf{x}';\ T,\ \theta] = -iS[X, y] + iS[X',\ y'] -$$
$$- ET - N\theta + B_i(\mathbf{x}_i, \mathbf{x}'_i; T, \theta). \quad \text{(A.9)}$$

Here, the nontrivial initial term B_i is

$$B_i = \frac{(X_i - X'_i)^2}{2T} - \frac{\omega}{1 - \exp(2\omega T + 2\theta)} \times$$
$$\times \left[\frac{1}{2}(y_i^2 + y_i'^2)(1 + \exp(2\omega T + 2\theta)) - \right.$$
$$\left. - 2 y_i y'_i \exp(\omega T + \theta) \right]. \quad \text{(A.10)}$$

In (A.8), $\mathbf{x}$ and $\mathbf{x}'$ are independent integration variables, while $\mathbf{x}'_f \equiv \mathbf{x}_f$, see Eq. (A.5).

2. The boundary value problem

For small λ, path integral (A.8) is dominated by a stationary point of the functional F. Therefore, to calculate the tunneling probability exponent, we extremize this functional with respect to all the integration variables $X(t)$, $y(t)$, $X'(t)$, $y'(t)$, T, and θ. We note that because of the limit $t_f - t_i \to +\infty$, the variation with respect to the initial and final values of the coordinates leads to boundary conditions imposed at asymptotic $t \to \pm\infty$, rather than at finite times t_i, t_f. We also note that the stationary points may be complex.

Variation of functional (A.9) with respect to the coordinates at intermediate times gives second-order equations of motion, in general complexified,

$$\frac{\delta S}{\delta X(t)} = \frac{\delta S}{\delta y(t)} = \frac{\delta S'}{\delta X'(t)} = \frac{\delta S'}{\delta y'(t)} = 0. \quad \text{(A.11a)}$$

The boundary conditions at the final time $t_f \to +\infty$ are obtained by extremization of F with respect to $X_f \equiv X'_f$ and $y_f \equiv y'_f$. These are

$$\dot{X}_f = \dot{X}'_f, \quad \dot{y_f} = \dot{y'_f}. \quad \text{(A.11b)}$$

It is convenient to write the conditions at the initial time (obtained by varying X_i, y_i, X'_i, and y'_i) in terms of the asymptotic quantities. At the initial time instant $t_i \to -\infty$, the system moves in the region $X \to -\infty$, well outside the range of the potential barrier. Equations (A.11a) in this region describe free motion of decoupled oscillators, and the general solution takes the form

$$X(t) = X_i + p_i(t - t_i),$$
$$y(t) = \frac{1}{\sqrt{2\omega}} \left[a \exp(-i\omega(t - t_i)) + \bar{a} \exp(i\omega(t - t_i)) \right],$$

and similarly for $X'(t)$ and $y'(t)$. For the moment, a and $\bar{a}$ are independent variables. In terms of the asymptotic variables X_i, p_i, a, $\bar{a}$, the initial boundary conditions become

$$\begin{aligned} p_i = p'_i &= -\frac{X_i - X'_i}{iT}, \\ a' + \bar{a}' &= a \exp(\omega T + \theta) + \bar{a} \exp(-\omega T - \theta), \\ a + \bar{a} &= a' \exp(-\omega T - \theta) + \bar{a}' \exp(\omega T + \theta). \end{aligned} \quad \text{(A.11c)}$$

Variation with respect to the Lagrange multipliers T and θ gives the relation between the values of E, N, and the initial asymptotic variables (where we use boundary conditions (A.11c)),

$$\begin{aligned} E &= \frac{p_i^2}{2} + \omega N, \\ N &= a\bar{a}. \end{aligned} \quad \text{(A.11d)}$$

Equations (A.11a)–(A.11d) constitute the complete set of saddle-point equations for the functional F.

The variables X' and y' originate from the conjugate amplitude $\mathcal{A}^*_{i'f}$ (see Eq. (A.5)), which suggests that they are complex conjugate to X and y. Indeed, the ansatz $X'(t) = X^*(t)$, $y'(t) = y^*(t)$ is compatible with boundary value problem (A.11). The Lagrange multipliers T and θ are then real, and problem (A.11) may be conveniently formulated on the contour $ABCD$ in the complex time plane (see Fig. 2).

We now have only two independent complex variables $X(t)$ and $y(t)$, which have to satisfy the classical equations of motion in the interior of the contour,

$$\frac{\delta S}{\delta X(t)} = \frac{\delta S}{\delta y(t)} = 0. \quad \text{(A.12a)}$$

The final boundary conditions (see Eq. (A.11b)) become the reality conditions for the variables $X(t)$ and $y(t)$ at the asymptotic part D of the contour,

$$\begin{aligned} &\operatorname{Im} X_f = 0, \quad \operatorname{Im} y_f = 0, \\ &\operatorname{Im} \dot{X}_f = 0, \quad \operatorname{Im} \dot{y}_f = 0, \end{aligned} \quad t \to +\infty. \quad \text{(A.12b)}$$

Seemingly complicated initial conditions (A.11c) simplify when written in terms of the time coordinate $t' = t + iT/2$ running along the part AB of the contour. We again write the asymptotic form of a solution, but now along the initial part AB of the contour,

$$X = X_0 + p_0(t' - t_i),$$

$$y = \frac{1}{\sqrt{2\omega}}\left[u\exp(-i\omega(t' - t_i)) + v\exp(i\omega(t' - t_i))\right].$$

In terms of X_0, y_0, u, and v, boundary conditions (A.11c) become

$$\operatorname{Im} X_0 = 0, \quad \operatorname{Im} p_0 = 0, \tag{A.12c}$$

$$v = u^* e^{\theta}.$$

Finally, we write Eqs. (A.11d) in terms of the asymptotic variables along the initial part of the contour,

$$\begin{aligned} E &= \frac{p_0^2}{2} + \omega N, \\ N &= \omega u v. \end{aligned} \tag{A.13}$$

These equations determine the Lagrange multipliers T and θ in terms of E and N. Alternatively, we can solve problem (A.12) for given values of T and θ and find the values of E and N from Eqs. (A.13), which is more convenient computationally.

Given a solution to problem (A.12), the exponent F is the value of functional (A.9) at this saddle point. We thus obtain expression (8) for the tunneling exponent. The exponent F is now expressed in terms of S_0 in Eq. (9), the action of the system integrated by parts. The nontrivial boundary term B_i, Eq. (A.10), is canceled by the boundary term coming from integration by parts. We note that we did not use constraints (A.13) to obtain formula (8), and we therefore still have to extremize (8) with respect to T and θ (see discussion in Sec. 2.2).

Classical problem (A.12) is conveniently called the T/θ boundary value problem. Equations (A.12b) and (A.12c) imply eight real boundary conditions for two complex second-order differential equations (A.12a). However, one of these real conditions is redundant: Eq. (A.12b) implies that the (conserved) energy is real, and therefore the condition $\operatorname{Im} p_0 \to 0$ is automatically satisfied (we note that the oscillator energy $E_{osc} = \omega u v = \omega e^{\theta} u u^*$ is real). On the other hand, system (A.12) is invariant under time translations along the real axis. This invariance is fixed, e.g., by requiring that $\operatorname{Re} X$ takes a prescribed value at a prescribed large negative time t_0' (we note that other ways may be used instead; in particular, for $E < E_1(N)$, it is convenient to impose the constraint $\operatorname{Re}\dot{X}(t = 0) = 0$). Together with the latter requirement, we have exactly eight real boundary conditions for the system of two complexified (i.e., four real) second-order equations.

APPENDIX B

A property of solutions of the T/θ problem in the case of over-barrier transitions

For given E and N, there is only one over-barrier classical solution, which is obtained in the limit $\epsilon \to 0$ of the regularized T/θ procedure. To see what singles out this solution, we analyze the regularized functional

$$F_\epsilon[q] = F[q] + 2\epsilon T_{int}[q], \tag{B.1}$$

where q denotes the variables $\mathbf{x}(t)$, $\mathbf{x}'(t)$ and T, θ together. The unregularized functional F has a valley of extrema $q^e(\varphi)$ corresponding to different values of the initial oscillator phase φ. Clearly, at small ϵ, the extremum of F_ϵ is close to a point in this valley with the phase extremizing $T_{int}[q^e(\varphi)]$,

$$\frac{d}{d\varphi} T_{int}[q^e(\varphi)] = 0. \tag{B.2}$$

Hence, the solution q_ϵ^e of the regularized T/θ boundary value problem tends to the over-barrier classical solution, with T_{int} extremized with respect to the initial oscillator phase.

Because $U_{int}(\mathbf{x}) > 0$, T_{int} is a positive quantity with at least one minimum. In normal situation, there is only one saddle point of F_ϵ, and hence solving the T/θ boundary value problem gives the classical solution with the time of interaction minimized.

APPENDIX C

Classically allowed transitions: a one-dimensional example

The difficulties with bifurcations of classical solutions emerge in quite a general class of quantum mechanical models. To illustrate this statement, we consider one-dimensional quantum mechanics, where the result is given by the well-known WKB formula. We show that the origin of the above difficulties can also be seen in one-dimensional model. Implementation of the regularization technique is explicit in the one-dimensional case. This makes it easy to see how our technique allows us to smoothly join the classical solutions relevant to the tunneling and allowed transitions.

Quantum mechanics of one degree of freedom involves only one variable $X(t)$ that describes motion of a particle with mass $m = 1$ through a potential barrier $U(X)$. The motion is free in the asymptotic regions $X \to \pm\infty$. The semiclassical calculation of the tunneling exponent is performed by solving the classical equation of motion

$$\frac{\delta S}{\delta X(t)} = 0$$

on the contour $ABCD$ in the complex time plane, with the condition that the solution is real in the asymptotic past (region A) and asymptotic future (region D). The relevant solutions tend to $X \to -\infty$ and $X \to +\infty$ in regions A and D, respectively. The auxiliary parameter T is related to the energy of the incoming state by the requirement that the energy of the classical solution equals to E. The exponent for the transition probability is

$$F = 2\,\mathrm{Im}\,S - ET. \qquad \text{(C.1)}$$

We note that these boundary conditions resemble the ones on the tunneling coordinate X in the two-dimensional system.

In quantum mechanics of one degree of freedom, the contour $ABCD$ may be chosen such that the points B and C are the turning points of the solution. Then the solution is also real at the part BC of the contour. Indeed, a real solution at the part BC of the contour oscillates in the upside-down potential, $T/2$ is equal to the half-period of oscillations, and the points B and C are the two different turning points, $\dot{X} = 0$. Continuation of this solution from the point C to the positive real times in accordance with the equation of motion corresponds to real-time motion, with zero initial velocity, towards $X \to +\infty$; the coordinate $X(t)$ stays real on the part CD of the contour. Likewise, the continuation back in time from the point B leads to a real solution in the part AB of the contour. The reality conditions are thus satisfied at A and D. The only contribution to F comes from the Euclidean part of the contour, and it can be checked that expression (C.1) reduces to

$$F(E) = 2\int\limits_{X_B}^{X_C} \sqrt{2(U(X) - E)}\, dX, \qquad \text{(C.2)}$$

which is the standard WKB result.

The solutions appropriate for the classically forbidden and classically allowed transitions apparently belong to different branches. As the energy approaches the height of the barrier U_0 from below, the amplitude of the oscillations in the upside-down potential decreases, while the period T tends to a finite value determined by the curvature of the potential at its maximum. On the other hand, the solutions for $E > U_0$ always run along the real time axis, and hence the parameter T is always zero. Therefore, the relevant solutions do not merge at $E = U_0$, and $T(E)$ has a discontinuity at $E = U_0$. The regularization technique of Sec. 3.1 removes this discontinuity and allows smooth transitions through the point $E = U_0$. The only difference with quantum mechanics of multiple degrees of freedom is that in the latter case, bifurcation points exist not only at the boundary of the region of classically allowed transitions, but also well inside the region of classically forbidden transitions (but still at $E > E_S$, see the Introduction and Sec. 2.3).

To illustrate the situation, we consider an exactly solvable model with

$$U(X) = \frac{1}{\mathrm{ch}^2\, X}.$$

We implement our regularization technique by formally changing the potential

$$U(X) \to e^{-i\epsilon} U(X), \qquad \text{(C.3)}$$

which leads to the corresponding change of the classical equations of motion. Here, ϵ is a real regularization parameter, the smallest parameter in the model. At the end of the calculations, we take the limit $\epsilon \to 0$.

We do not change the boundary conditions in our regularized classical problem, i.e., we still require $X(t)$ to be real in the asymptotic future on the real time axis and $X(t')$ to be real as $t' \to -\infty$ on part A of the contour $ABCD$. Then the conserved energy is real. The sphaleron solution $X(t) = 0$ now has a complex energy (because the potential is complex). Hence, the solutions of our classical boundary value problem necessarily avoid the sphaleron, and we can expect that the solutions behave smoothly in energy.

The general solution of the regularized problem is

$$\sqrt{\frac{E}{e^{-i\epsilon} - E}}\,\mathrm{sh}\, X = -\,\mathrm{ch}\left(\sqrt{2E}(t - t_0)\right),$$

where t_0 is the integration constant. The value of $\mathrm{Im}\, t_0$ is fixed by the requirement that $\mathrm{Im}\, X = 0$ at positive time $t \to +\infty$,

$$\mathrm{Im}\, t_0 = \frac{T}{2} - \frac{1}{2\sqrt{2E}}\arg[e^{-i\epsilon} - E].$$

The residual parameter $\mathrm{Re}\, t_0$ represents the real-time translational invariance present in the problem. The condition that the coordinate X is real on the initial

part AB of the contour gives the relation between T and E,

$$\frac{T}{2} = \frac{1}{\sqrt{2E}} \left\{ \pi + \arg\left(e^{-i\epsilon} - E\right) \right\}. \qquad \text{(C.4)}$$

For $\epsilon = 0$ and $E < 1$, the original unregularized result $T/2 = \pi/\sqrt{2E}$ is reproduced.

We now analyze what happens in the regularized case in the vicinity of the would-be special value of energy, $E = E_S \equiv 1$. It is clear from Eq. (C.4) that T is now a smooth function of E. Away from $E = 1$, Eq. (C.4) can be written as

$$\frac{T}{2} = \begin{cases} \dfrac{\pi}{\sqrt{2E}}, & \text{forbidden region, } 1-E \gg \epsilon \\ \dfrac{\epsilon}{\sqrt{2E}(E-1)}, & \text{allowed region, } E-1 \gg \epsilon. \end{cases} \qquad \text{(C.5)}$$

Deep enough in the region of forbidden transitions, where $1 - E \gg \epsilon$, the argument in Eq. (C.4) is nearly zero and we return to the original tunneling solution. When E crosses the region of size of the order of ϵ around $E = 1$, the argument rapidly changes from $O(\epsilon)$ to $-\pi$, and hence $T/2$ changes from $\pi/\sqrt{2}$ to nearly zero. Thus, at $E > 1$, we obtain a solution that is very close to the classical over-barrier transition, and the contour is also very close to the real axis. This is shown in Fig. 9. We conclude that at small but finite ϵ, the classically allowed and classically forbidden transitions merge smoothly.

For $E < 1$, the limit $\epsilon \to 0$ is straightforward. For $E > 1$, a somewhat more careful analysis of the limit $\epsilon \to 0$ is needed. It follows from Eq. (C.5) that the limit $\epsilon \to 0$ with a constant finite $T < \pi\sqrt{2}$ leads to solutions with $E = 1$. Classical over-barrier solutions of the original problem with $E > E_S \equiv 1$ are obtained in the limit $\epsilon \to 0$ if T also tends to zero while $\tau = T/\epsilon$ is kept finite. Different energies correspond to different values of τ. This is what one expects — classical over-barrier transitions are described by the solutions on the contour with $T \equiv 0$.

REFERENCES

1. Z. Huang, T. Feuchtwang, P. Cutler, and E. Kazes, Phys. Rev. A **41**, 32 (1990).
2. S. Takada and H. Nakamura, J. Chem. Phys. **100**, 98 (1994).
3. W. Miller, J. Chem. Phys. **53**, 3578 (1970).
4. W. Miller and T. George, J. Chem. Phys. **56**, 5668 (1972).
5. T. George and W. Miller, J. Chem. Phys. **57**, 2458 (1972).
6. W. H. Miller, Adv. Chem. Phys. **25**, 69 (1974).
7. M. Wilkinson, Physica D **21**, 341 (1986).
8. M. Wilkinson and J. Hannay, Physica D **27**, 201 (1987).
9. S. Takada, P. Walker, and M. Wilkinson, J. Chem. Phys. **52**, 3546 (1995).
10. S. Takada, J. Chem. Phys. **104**, 3742 (1996).
11. G. F. Bonini, A. G. Cohen, C. Rebbi, and V. A. Rubakov, E-print archives quant-ph/9901062.
12. G. F. Bonini, A. G. Cohen, C. Rebbi, and V. A. Rubakov, Phys. Rev. D **60**, 076004 (1999).
13. V. A. Rubakov, D. T. Son, and P. G. Tinyakov, Phys. Lett. B **287**, 342 (1992).
14. A. N. Kuznetsov and P. G. Tinyakov, Phys. Rev. D **56**, 1156 (1997).
15. F. Bezrukov, C. Rebbi, V. Rubakov, and P. Tinyakov, E-print archives hep-ph/0110109.
16. F. Bezrukov, D. Levkov, C. Rebbi et al., Phys. Rev. D **68**, 036005 (2003).
17. A. M. Perelomov, V. S. Popov, and M. V. Terent'ev, Zh. Eksp. Teor. Fiz. **51**, 309 (1966).
18. V. S. Popov, V. Kuznetsov, and A. M. Perelomov, Zh. Eksp. Teor. Fiz. **53**, 331 (1967).
19. N. Makri and W. Miller, J. Chem. Phys. **89**, 2170 (1988).
20. K. Thompson and N. Makri, J. Chem. Phys. **110**, 1343 (1999).
21. K. Kay, J. Chem. Phys. **107**, 2313 (1997).
22. N. Maitra and E. Heller, Phys. Rev. Lett. **78**, 3035 (1997).
23. W. Miller, J. Phys. Chem. A **105**, 2942 (2001).
24. A. N. Kuznetsov and P. G. Tinyakov, Mod. Phys. Lett. A **11**, 479 (1996).
25. M. Davis and E. Heller, J. Chem. Phys. **75**, 246 (1981).

26. E. Heller and M. Davis, J. Phys. Chem. **85**, 309 (1981).

27. E. Heller, J. Phys. Chem. **99**, 2625 (1994).

28. T. Banks, G. Farrar, M. Dine et al., Nucl. Phys. B **347**, 581 (1990).

29. V. I. Zakharov, Phys. Rev. Lett. **67**, 3650 (1991).

30. G. Veneziano, Mod. Phys. Lett. A **7**, 1661 (1992).

31. V. A. Rubakov, E-print archives hep-ph/9511236.

32. V. A. Rubakov and P. G. Tinyakov, Phys. Lett. B **279**, 165 (1992).

33. F. R. Klinkhamer and N. S. Manton, Phys. Rev. D **30**, 2212 (1984).

34. S. Y. Khlebnikov, V. A. Rubakov, and P. G. Tinyakov, Nucl. Phys. B **367**, 334 (1991).

35. C. Rebbi and R. Singleton, E-print archives hep-ph/9502370.